 CMES, vol.56, no.3, pp.231-247, 2010

Numerical Prediction of Young's and Shear Moduli of Carbon Nanotube Composites Incorporating Nanoscale and Interfacial Effects

G.I. Giannopoulos[1], **S.K. Georgantzinos**[2], **D.E. Katsareas**[2]
N.K. Anifantis[2]

Abstract: A hybrid finite element formulation, combining nanoscopic and macroscopic considerations is proposed, for the prediction of the elastic mechanical properties of single walled carbon nanotube (SWCNT)-based composites. The nanotubes are modeled according to the molecular mechanics theory via the use of spring elements, while the matrix is modeled as a continuum medium. A new formulation concerning the load transfer between the nanotubes and matrix is proposed. The interactions between the two phases are implemented by utilizing appropriate stiffness variations describing a heterogeneous interfacial region. A periodic distribution and orientation of the SWCNTs is considered. Thereupon, the nanocomposite is modeled using a three dimensional finite element unit cell, which is subjected to longitudinal as well as transverse loadings in order to obtain the mechanical properties in these directions. The Halpin-Tsai equations are used to extract the mechanical properties for randomly oriented SWCNTs. The formulation is validated through comparison of the predicted mechanical responses to corresponding solutions, obtained from the literature.

Keywords: Carbon nanotube, Finite element method, Mechanical properties, Interface, Nanocomposite.

1 Introduction

As there is a demand in modern technological applications for superior composites, innovative reinforcements having superior properties should be introduced. Such reinforcements could be found in the field of nanotechnology. Since carbon-carbon

[1] Department of Mechanical Engineering, Technological and Educational Institute of Patras, GR-26334, Patras, Greece.
[2] Machine Design Laboratory, Department of Mechanical Engineering and Aeronautics, University of Patras, Rion 26500, Greece.

covalent bonds are one of the strongest in nature, a nanostructure based on a perfect arrangement of these bonds would produce a remarkably strong reinforcement.

Due to their molecular structure, carbon nanotubes (CNTs), first recognized by Iijima [Iijima (2001)], are the stiffest and strongest known nano-reinforcing agents, having also remarkable electronic and conductive properties and many other unique characteristics [Thostenson, Ren and Chou (2001)]. Development of CNT-based composites could demonstrate the advanced structural properties of the individual nanotubes. SWCNT reinforced composite materials, with significant enhancement in mechanical properties, have already been fabricated [Mamedv, Kotov, Prato, Guldi, Wicksted and Hirsch (2002)]. Recent experimental investigations indicate that significant improvements in the elastic properties of polymeric materials can be achieved by using as reinforcement carbon nanotubes of even small volume fractions [Ajayan and Tour (2007); Kueseng and Jacob (2006); Atieh, Girun, Mahdi, Tahir, Guan, Alkhatib, Ahmadun and Baik (2006)]. Since the experimental study of CNT composites is often an expensive and complicated task, computational modeling could be a significant aid in the specific research area.

Atomic modeling of carbon-based nanostructures has attracted the attention of several researchers [Brenner, Shederova, Areshkin, Schall and Frankland (2002); Chen, Cheng and Hsu (2007); Wu, Chou, Han and Chiang (2009)]. Molecular dynamics (MD) [Frankland, Harik, Odegard, Brenner and Gates(2003); Zou, Ji, Feng and Gao (2006); Han and Elliott (2007); Namilae, Chandra, Srinivasan, Chandra (2007);] and continuum mechanics [Chen and Liu (2004); Seidel and Lagoudas (2006); Ashrafi and Hubert (2006); Liu and Chen (2003); Araújo and Gray (2008); Guz, Rushchitsky, Guz (2008); Guz, Dekret (2009); Wang, Yao (2009)] based approaches have been adopted to simulate CNT composite behavior. Due to their computational cost, MD approaches are restricted to small length and time scale problems while continuum mechanics approaches fail to incorporate the nanostructural effects of the CNT. A micromechanical based method linking MD and continuum mechanics approaches has been recently proposed [Odegard, Gates, Wise, Park and Siochi (2003)]. The performance of CNT-based composites is greatly influenced by the interface, which has different properties from those of the matrix and the CNT. Generally, the three main mechanisms of interfacial load transfer are micromechanical interlocking, chemical bonding and the van der Waals interactions between the matrix and the reinforcements. Al-Ostaz [Al-Ostaz, G. Pal, Mantena and Cheng (2008)] investigated SWCNT-polymer interface interactions in nanoscale via MD. To represent the CNT-polymer load transfer characteristics and consequently the interface between the CNTs and the polymer, Frankland et al. [Frankland, Caglar, Brenner and Griebel (2002)] employed just van der Waals forces. Saber-Samadari and Khatibi [Saber-Samandari and Khatibi (2006)] con-

sidered a continuum interfacial zone with variable elastic modulus to investigate a CNT composite via a unit cell method. However, in the specific study all phases including CNTs were assumed as continuum.

A finite element formulation, based on micromechanical analysis, is proposed for the evaluation of the elastic mechanical behavior of a polymer matrix, filled with short SWCNTs. Concerning nanotube modeling [Giannopoulos, Kakavas and Anifantis (2008)], the method utilizes the three dimensional atomistic microstructure of the nanotube, defining nodes at the corresponding atomic positions of carbon atoms. Appropriate spring elements, which interconnect the atoms, incorporate directly the potential energies provided by molecular theory and therefore simulate accurately the interatomic interactions [Rappe, Casewit, Colwell, Goddard and Skiff (1992)]. In contrast, the matrix is considered as a continuum medium. In addition, the load transfer between the nanotubes and the matrix is modeled by special joint elements of variable stiffness. In this way, a heterogenous interface is simulated. The advantage of the proposed hybrid method is that it utilizes macroscopic properties in order to describe the matrix and interface behavior. Detailed representation of the molecular nanostructure is avoided, making the proposed formulation attractive and simultaneously, significant reductions in computational cost and complexity is achieved. Predicted results regarding the nanocomposite mechanical properties are presented and compared to solutions obtained from the literature. The reinforcing ability of SWCNTs is evaluated.

2 Numerical model

2.1 Micromechanical analysis

A composite with homogenously distributed SWCNTs is assumed. It is considered that all SWCNTs have the same dimensions and orientation and that their edges are capped. The microstructure of the nanotube is developed around a mean diameter $d_n = 2r_n$. The reinforcement length is ℓ_n. Its thickness is indirectly considered and typically taken equal to $t_n = 0.34$nm. It is assumed that the longitudinal distances, between neighboring reinforcement ends, are equal to the corresponding transverse distances and equal to d. The last condition in conjunction with the known volume fraction V_{fr} , diameter d_n and length l_n of SWCNT are sufficient to lead to the complete geometric definition of the problem. Due to the symmetry of the periodic distribution, only the representative repeated unit cell of Fig. 1 is modeled. In this figure, one quarter of the matrix is removed for clarity. An orthogonal Cartesian coordinate system is used as reference with x, y and z axes, aligned with the main dimensions of the unit cell. The longitudinal axis of the reinforcement is aligned with the uniaxial loading direction (Fig. 1).

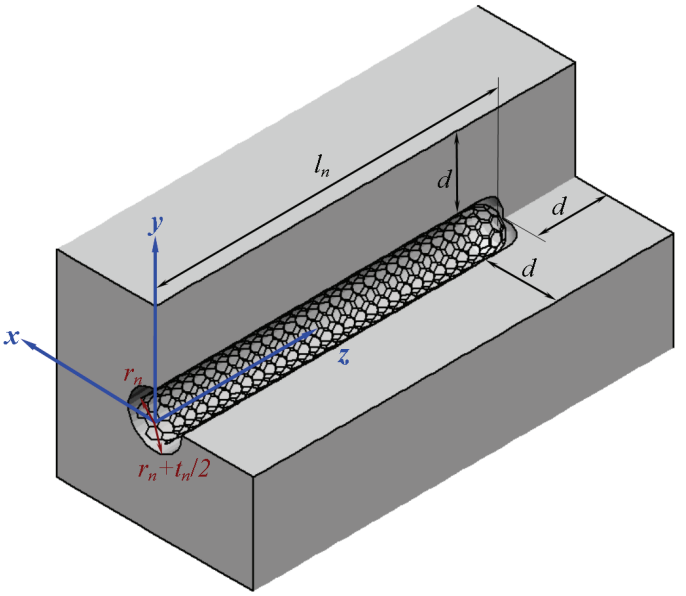

Figure 1: Representative unit cell of the nanocomposite.

The volume fraction of the CNT in the composite is:

$$V_{fr} = \frac{V_n}{V_m + V_n} \tag{1}$$

Small volume fractions are considered, so that a negligible interaction between adjacent nanotubes can be assumed. In order to determine the longitudinal and transverse elastic properties of the composite, by using the unit cell model, appropriate boundary conditions must be implemented. For the calculation of the longitudinal elastic modulus $E_L = E_z$ a uniform displacement $u_z = \Delta z$ is applied on the boundary $z = l_n + d$. The symmetry constraint $u_z = 0$ is applied on the boundary $z = 0$, whereas the boundaries $x = \pm(d + r_n + t_n/2)$ and $y = \pm(d + r_n + t_n/2)$ are kept parallel to their original shape by nodal coupling (this is required, as shear stresses on these boundaries must be zero due to symmetry). The longitudinal elastic modulus E_L of the composite is computed from average stress σ_z, obtained from the sum of reactions and average strain ε_z on $z = l_n + d$:

$$E_L = \frac{\sigma_z}{\varepsilon_z} = \frac{\frac{\sum_{i=1}^{n} (-^i f_z)}{(2d+d_n+t_n)^2}}{\frac{\Delta z}{l_n+d}} \tag{2}$$

where ${}^{i}f_z$ is the reaction in the direction z at node i, which belongs on the boundary $z = l_n + d$ and n is the total number of nodes that belong in the specific boundary.

Similarly, in order to compute the transverse elastic modulus $E_T = E_x = E_y$ a uniform displacement $u_x = \Delta x$ is applied on the boundary $x = d + r_n + t_n/2$, while the constraint $u_x = 0$ is imposed on the boundary $x = -(d + r_n + t_n/2)$. In addition, the boundaries $y = \pm(d + r_n + t_n/2)$ and $z = l_n + d$ are constrained to remain parallel to their original configuration. Finally, once more the symmetry constraint $u_z = 0$ is applied on the boundary $z = 0$. The transverse elastic modulus E_T of the composite is calculated from average normal reaction on the face $x = d + r_n + t_n/2$:

$$E_T = \frac{\sigma_x}{\varepsilon_x} = \frac{\frac{\sum_{i=1}^{n}(-{}^{i}f_x)}{(2d+d_n+t_n)(l_n+d)}}{\frac{\Delta x}{(2d+d_n+t_n)}} \tag{3}$$

where ${}^{i}f_x$ denotes the reaction along the direction x at node i, belonging on the face $x = d + r_n + t_n/2$, while n is the sum of the nodes belonging on the corresponding face.

After computing the elastic modulus E_L and E_T, predictions concerning the randomly oriented SWCNTs are performed, by using the following Halpin-Tsai relationships for randomly oriented short fiber composites [Mallick (1988)]:

$$E_{rand} = \frac{3}{8}E_L + \frac{5}{8}E_T \tag{4}$$

$$G_{rand} = \frac{1}{8}E_L + \frac{1}{4}E_T \tag{5}$$

where E_{rand} and G_{rand} are the elastic and shear modulus of a composite with randomly distributed short reinforcements, respectively.

2.2 Representation of SWCNT mechanical behavior

In contrast with a traditional carbon fiber, the mechanical performance of a SWCNT is strongly dependent on its atomistic nanostructure and therefore it is essential to be implemented into the proposed model [Giannopoulos, Kakavas and Anifantis (2008)]. According to the method adopted, the SWCNT is developed around its mean radius r_n. Specifically, the nanotube is considered as a space frame structure, in which the carbon atoms are represented by nodes. Their position in three-dimensional space, for a particular (p,q) SWCNT is established via the following transformation equation [Koloczek, Young-Kyun and Burian (2001)]:

$$(x,\ y,\ z) = \left(r_n \cos\left(\frac{x'}{r_n}\right),\ r_n \sin\left(\frac{x'}{r_n}\right),\ y'\right) \tag{6}$$

where (x', y') represents the original coordinate system of a graphene sheet and (x, y, z) represents the new coordinate system of the tube. The body of the tubular shell is mainly made of hexagonal rings of carbon atoms, whereas the ends are capped by a dome-shaped half-fullerene molecule made of hexagonal and pentagonal rings. Details about the carbon atom positions on the capped edges of SWCNTs can be found elsewhere [Reich, Li and Robertson (2005)].

The nodes that arise by using the above equation are properly connected with linear spring elements, which simulate the potential energy of the interatomic interactions [Rappe, Casewit, Colwell, Goddard and Skiff (1992)], depicted in Fig. 2. The total potential energy, omitting the electrostatic interactions between carbon atoms which have minor effect, is [Gelin (1994)]:

$$U = \sum U_r + \sum U_\theta + \sum U_\tau = \sum \frac{1}{2} k_r (\Delta r)^2 + \sum \frac{1}{2} k_\theta (\Delta\theta)^2 + \sum \frac{1}{2} k_\tau (\Delta\varphi)^2 \tag{7}$$

where U_r represents the energy due to bond stretching, U_θ the energy due to bond angle bending and U_τ the energy due to torsion. The terms k_r, k_θ and k_τ are the bond stretching, bond angle bending and torsional resistance force constants, respectively, while Δr, $\Delta\theta$ and $\Delta\varphi$ represent the bond length and bond angle variations, respectively. In order to represent the bond stretching interaction between carbon atoms, a linear spring element of stiffness k_r is utilized while a torsional linear spring element of stiffness k_τ is utilized for the representation of torsional interaction. For simplicity reasons, the bond angle bending interaction is simulated by the use of an equivalent straight spring element, connecting the opposite atoms-nodes of the C-C-C nanostructure, as Fig. 2 shows. It is easy to prove that for small deformations its stiffness is:

$$k_b = \frac{k_\theta}{(a_{c-c})^2 - 0.25(l_{c-c-c})^2} \tag{8}$$

where $a_{c-c} = 0.1421\,\text{nm}$ is distance between two neighboring carbon atoms while l_{c-c-c} is the distance between two opposite atoms in a C-C-C nanostructure.

The spring elements as well as their stiffness values, used in the analysis are depicted in Fig. 2. As it can be seen, the a elements simulate stretching and torsion interaction while the b elements represent the angle bending interaction. These elements are two-noded and have 3 degrees of freedom per node (three translations), that are expressed in the global coordinate system. The two nodes of these elements are connected with three translation springs. Theses springs are situated according to the local coordinate system of the element $(\bar{x}, \bar{y}, \bar{z})$. The $\bar{x}$-axis of the specific local coordinate system always coincides with the line that connects the two nodes. Each finite element is characterized by six values of stiffness, corresponding to the aforementioned translation and rotation springs: $(k_{\bar{x}}, k_{\bar{y}}, k_{\bar{z}}, k_{rot\bar{x}}, k_{rot\bar{y}}, k_{rot\bar{z}})$

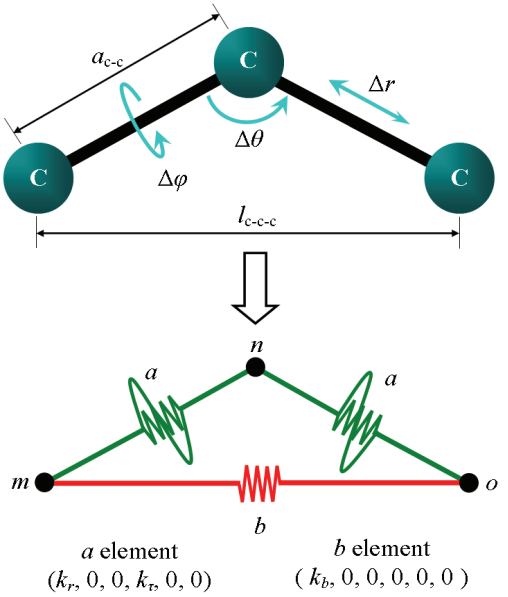

Figure 2: Interatomic interactions and corresponding finite element model.

2.3 Representation of matrix mechanical behavior

The matrix can be modeled discretely, by taking into consideration its molecular structure. However, this would increase significantly the computational cost, as well as the complexity of the whole model. Therefore, the matrix is regarded as a continuum isotropic elastic medium of elastic modulus E_m and Poisson's ratio ν_m. Linear three-dimensional hexahedral isoparametric elements are used for the discretization of the matrix (annotated hereafter as s elements). These elements have eight nodes with three degrees of freedom per node (three translations) and a linear strain variation displacement mode.

2.4 Representation of interface mechanical behavior

Between the matrix and the SWCNTs, occur complicated phenomena such chemical bonding and van der Waals interactions which depend on the nature of the interacting atoms and relative distances. Since it is difficult to implement implicitly such phenomena in a numerical model, a computationally efficient formulation capable of representing approximately an overall interfacial mechanical response should be adopted.

As it was previously mentioned, the nanostructure of a carbon nanotube is devel-

oped around a mean diameter, while its thickness is considered indirectly. Therefore, from a physical point of view, it is assumed that the interfacial interactions take place along a radial distance equal to $t_n/2$. Due to the atomistic modelling of SWCNTs, a discrete modelling of the interfacial region is adopted. Two-noded interfacial joint elements (annotated hereafter as j elements), are employed. As Fig. 3 illustrates, these elements interconnect radially the atoms-nodes of the nanotube with corresponding nodes, belonging to the inner surface of the matrix.

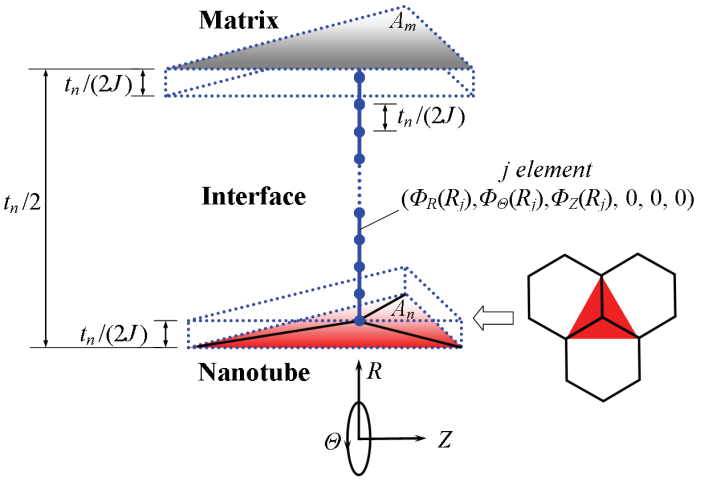

Figure 3: Finite element model of interfacial interactions.

A series of J elements of equal lengths $t_n/(2J)$, is used to span the distance $t_n/2$. The translation stiffnesses, along the three directions of these elements are defined according to a local cylindrical coordinate system $(R,\ \Theta,\ \mathrm{Z})$, positioned at the center of the SWCNT perimeter. It is assumed that their values are functions of the radial coordinate R:

$$k_i = \Phi_i(R) \tag{9}$$

where $i = R,\ \Theta,\ \mathrm{Z}$. The following step is to define the lower and upper bounds for functions $\Phi_i(R)$, by taking into consideration their minimum and maximum allowed values. The radial reaction f_R, produced by the joint above the SWCNT, for a ΔR deformation, is according to Eq. (9):

$$f_R = \Phi_R(R_1)\Delta R \tag{10}$$

where R_1 denotes the radial position of the joint element and is equal to:

$$R_1 = r_n + t_n/(2J) \tag{11}$$

Eq. (10) may take the form:

$$\frac{f_R}{A_n} = \frac{\Phi_R(R_1)(t_n/2J)}{A_n}\frac{\Delta R}{(t_n/2J)} \tag{12}$$

where A_n indicates the mean surface area of the nanotube affected by the joint, given by the equation:

$$A_n = \frac{2\pi r_n l_n}{n_c} \tag{13}$$

where n_c is the total number of carbon atoms of the tube. Eq. (12) may be equivalently written as:

$$\sigma_R = \frac{\Phi_R(R_1)t_n n_c}{4\pi J r_n l_n}\varepsilon_R \tag{14}$$

where σ_R and ε_R denote radial stress and strain, respectively. It is coherent to assume that the radial elastic modulus of the interface, exactly above the reinforcement, is equal to the corresponding radial elastic modulus of the nanotube E_{Rn}. Therefore, from Eq. (14) the following constrained equation is obtained:

$$\Phi_R(R_1) = \frac{4\pi J r_n l_n}{t_n n_c}E_{Rn} \tag{15}$$

A similar constrain equation can be obtained for function Φ_Θ. The circumferential reaction f_Θ, produced by the joint above the SWCNT for a $\Delta\Theta$ deformation, is:

$$f_R = \Phi_R(R_1)\Delta R \tag{16}$$

or

$$\frac{f_\Theta}{A_n} = \frac{\Phi_R(R_1)t_n n_c}{4\pi J r_n l_n}\frac{\Delta\Theta}{(t_n/2J)} \tag{17}$$

For small strains the above equation becomes:

$$\tau_\Theta = \frac{\Phi_R(R_1)t_n n_c}{4\pi J r_n l_n}\gamma_R \tag{18}$$

where τ_Θ and γ_Θ denote circumferential shear stress and strain, respectively. The above equation leads to the following constrain equation:

$$\Phi_\Theta(R_1) = \frac{4\pi J r_n l_n}{t_n n_c} G_{\Theta n} \tag{19}$$

where $G_{\Theta n}$ is the circumferential shear modulus of the SWCNT. Accordingly, function Φ_Z becomes:

$$\Phi_Z(R_1) = \frac{4\pi J r_n l_n}{t_n n_c} G_{Zn} \tag{20}$$

where G_{Zn} is the longitudinal shear modulus of the SWCNT. In a similar manner and by making the same considerations for the joint element located exactly below the matrix material, the following equations are obtained:

$$\Phi_R(R_2) = \frac{4\pi J (r_n + t_n/2) l_n}{t_n n_c} E_{Rm} \tag{21}$$

$$\Phi_\Theta(R_2) = \frac{4\pi J (r_n + t_n/2) l_n}{t_n n_c} G_{\Theta m} \tag{22}$$

$$\Phi_Z(R_2) = \frac{4\pi J (r_n + t_n/2) l_n}{t_n n_c} G_{Zm} \tag{23}$$

where E_{Rm}, $G_{\Theta m}$ and G_{Zm} are the radial elastic modulus, the circumferential shear modulus and longitudinal shear modulus of the matrix material, respectively. Finally R_2 denotes the radial position of the specific joint element and is given by the following equation:

$$R_2 = r_n + t_n/2 - t_n/(2J) \tag{24}$$

It has to be noted that the above stiffness variations are not appropriate for the capped edges of the tube. Therefore, in order to describe the interface surrounding the capped edges, the above functions are expressed with respect to an appropriate local spherical coordinate system positioned at the centre of the cap.

Summarizing, a heterogeneous interface is modeled in a discrete manner by introducing joint elements of variable stiffness properties. Their mechanical response is prescribed by user-defined functions, along the three dimensions of a local coordinate system. These functions, from physical point of view, are set to be bounded exclusively by macroscopic parameters of the two phases surrounding the interface.

3 Results and discussion

3.1 SWCNT properties

The armchair (6,6) SWCNTs is considered as reinforcement with a radius equal to $r_n = 0.40709$nm. In order to represent the mechanical interfacial behavior, as Eqs. (15), (19) and (20) imply, some macroscopic material data i.e. E_{Rn}, $G_{\Theta n}$ and G_{Zn} of the considered SWCNT are required. For this reason, initially the uncapped (6,6) SWCNT is individually modeled. A length equal to $l_n = 10$nm is selected. The SWCNT is analyzed with reference to the local cylindrical coordinate system (R, Θ, Z), mentioned earlier. The bond stretching and bond angle bending resistance force constants are taken equal to $k_r = 6.52 \times 10^{-7}$ Nnm^{-1}, and $k_\theta = 8.76 \times 10^{-10}$, respectively [Giannopoulos, Kakavas and Anifantis (2008)].

In order to compute the radial elastic modulus of the SWCNT E_{Rn}, a radial force f_R is imposed at each one of its nodes. The E_{Rn} can then be calculated via equation:

$$E_{Rn} = \frac{\sigma_R}{\varepsilon_R} = \frac{\frac{n_c f_R}{2\pi r_n l_n}}{\frac{\Delta R}{r_n}} \tag{25}$$

In order to compute the circumferential shear modulus of the SWCNT G_{Rn}, the Θ degree of freedom of the nodes at $Z = 0$ is restrained, while a circumferential force f_Θ is applied uniformly on each node that belongs to the $Z = l_n$ plane. The shear module G_{Rn} of the nanotube is computed from the reaction torgue M_Z acting, in the restrained end:

$$G_{Rn} = \frac{M_Z l_n}{S\Delta\Theta} = \frac{n'_c f_\Theta r_n l_n}{\frac{\pi}{2}\left(\left(r_n + \frac{t_n}{2}\right)^4 - \left(r_n - \frac{t_n}{2}\right)^4\right)\Delta\Theta} \tag{26}$$

where S is the polar moment of inertia of the cross sectional area of the tube and n'_c is the number of edge nodes of the tube.

In order to compute the longitudinal shear modulus of the SWCNT G_{Zn}, only half of the tube, from $\Theta = 0$ to $\Theta = \pi$, is modeled. R and Θ degrees of freedom of all nodes an Z degree of freedom of nodes belonging to plane $\Theta = \pi$, are constrained. A longitudinal displacement variation $R_i \Delta Z$ is applied to nodes, belonging to planes $Z = 0$ and $Z = l_n$, where R_i is the radial coordinate of node i. The shear module G_{Zn} of the nanotube is computed using the following relationship:

$$G_{Zn} = \frac{\tau_Z}{\gamma_Z} = \frac{\frac{\sum_{i=1}^{n''_c} (-^i f_Z)}{l_n t_n}}{\frac{\Delta Z}{r_n}} \tag{27}$$

where ${}^{i}f_Z$ is the longitudinal reaction of node i, belonging to plane $\Theta = \pi$ and $n"_c$ is the total number of nodes belonging to the same plane.

The obtained values using the above techniques are $E_{Rn} = 1515$GPa, $G_{\Theta n} = 336.5$GPa and $G_{Zn} = 547.3$GPa.

3.2 Composite properties

In this section the computed elastic moduli, of a (6,6) capped SWCNT/polymer nanocomposite, are presented in terms of nanotube length, volume fraction and orientation. The thermoplastic polyamide LaRC-SI [Odegard, Gates, Wise, Park and Siochi (2003)] is used as matrix material. The elastic modulus and Poisson's ratio of this material are $E_m = E_{Rm} = 3.8$GPa and $\nu_m = 0.4$, respectively. The shear modulus of the polymer is:

$$G_m = G_{\Theta m} = G_{Zm} = \frac{E_m}{2(1+\nu_m)} = 1.357\text{GPa} \tag{28}$$

In order to define the interface properties, a set of linear functions are selected having the form:

$$\Phi_i(R) = \alpha_i R + \beta_i \tag{29}$$

where $i = R$, Θ, Z and α_i, β_i are constants that must be determined. Since the macroscopic properties E_{Rn}, $G_{\Theta n}$, G_{Zn},E_{Rm}, $G_{\Theta m}$, and G_{Zm} are known, the interfacial stiffness variations, with reference to the local coordinate system (R, Θ, Z), can be fully defined (evaluations of α_i, β_i constants) by substituting Eqs. (15), (19)-(23) and (29). At the capped edge region these variations are transformed with respect to the spherical local coordinate system mentioned previously. A set of $J = 10$ joint elements is used along the radial direction. The selection of this number has been made after convergence tests. During these tests it was proved that for $J > 10$, elastic properties of same magnitude were produced.

A representative finite element model of the unit cell containing a capped (6,6) SWCNT is illustrated in Fig. 4.

Before extracting the numerical data, numerous convergence tests have been conducted in order to select the proper mesh density concerning the matrix material. The variation of longitudinal and transverse elastic moduli versus SWCNT length, for 1% volume fraction is given in Fig. 5. The variation of longitudinal and transverse elastic moduli versus volume fraction, for a SWCNT length equal to 10nm, is given in Fig. 6.

The isotropic elastic and shear modulus of a composite, with randomly aligned SWCNTs, is semi-analytically obtained, by substituting the numerically predicted

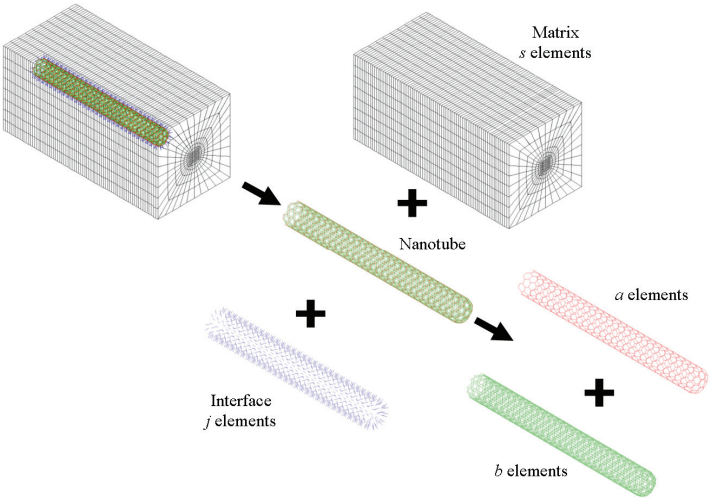

Figure 4: Finite element model of the unit cell.

values of longitudinal and transverse elastic moduli, into Eq. (4) and (5), respectively.

Fig. 7 presents the elastic and shear modulus of the composite with randomly aligned tubes, for 1% volume fraction versus reinforcement length. Fig. 8 depicts the elastic and shear modulus of the composite with randomly aligned tubes of 10nm length versus volume fraction.

Generally, for the aligned SWCNT/ LaRC-SI composites, the longitudinal elastic modulus increases significantly, as the reinforcement length and volume fraction increases, while the transverse elastic modulus remains almost constant. For the aligned SWCNT/ LaRC-SI, the increase of the reinforcement length and volume fraction leads to a less prominent increase of both isotropic elastic and shear moduli. In general, a satifactory agreement is observed between preictions obtained using the proposed method and results presented by Odegard et al. [Odegard, Gates, Wise, Park and Siochi (2003)].

4 Conclusions

In the present study a hybrid numerical method capable of predicting the mechanical response of CNT based composites has been developed. The method combines the discrete nature of the CNT and the macroscopic mechanical response of the matrix. Furthermore, it utilizes a discrete representation of the interface, assuming appropriate interfacial stiffness variations defined by functions of radius, bounded

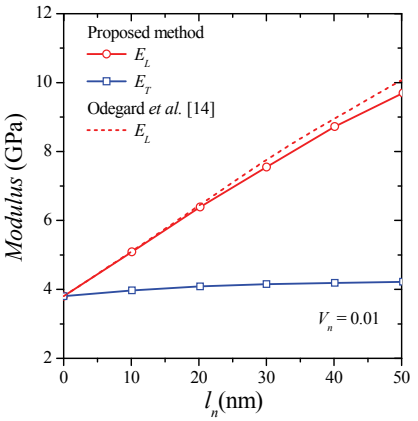

Figure 5: Longitudinal and transverse moduli of aligned capped (6,6) SWCNT/ LaRC-SI nanocomposite versus nanotube length, for 1% volume fraction.

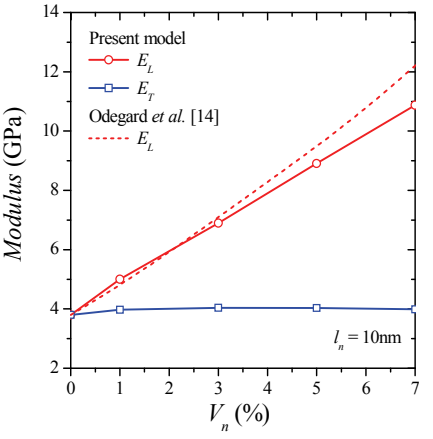

Figure 6: Longitudinal and transverse moduli of aligned capped (6,6) SWCNT/ LaRC-SI nanocomposite versus nanotube length, for 1% volume fraction.

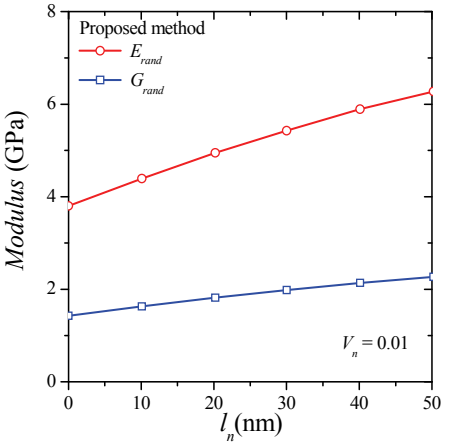

Figure 7: Elastic and shear moduli of random capped (6,6) SWCNT/ LaRC-SI nanocomposite versus nanotube length, for 1% volume fraction.

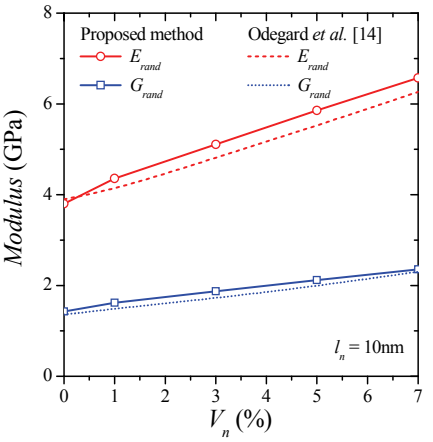

Figure 8: Elastic and shear moduli of random capped (6,6) SWCNT/ LaRC-SI nanocomposite versus volume fraction, for 10nm long nanotubes.

by the macroscopic properties of the two phases.

This hybrid method reduces significantly the computational cost and modeling complexity since it uses macroscopic representation for the matrix and the interface. Therefore the input of detailed data concerning the matrix atomistic structure, possible covalent bonding and van der Waals interactions between the two phases is avoided. The method has been tested successfully for a CNT-LaRC-SI composite by comparison with other corresponding solutions available in the literature.

References

Ajayan, P. M.; Tour, J. M. (2007): Nanotube composites. *Nature*, vol. 447, pp. 1066-1068.

Al-Ostaz, A.; Pal, G.; Mantena, P. R.; Cheng, A. (2008): Molecular dynamics simulation of SWCNT-polymer nanocomposite and its constituents. *Journal of Materials Science*, vol. 43, pp. 164-173.

Araújo, F. C.; Gray, L. J. (2008): Evaluation of effective material parameters of CNT-reinforced composites via 3D BEM. *CMES: Computer Modeling in Engineering and Sciences*, vol. 24, no. 2, pp. 103-121.

Ashrafi, B.; Hubert, P. (2006): Modeling the elastic properties of carbon nanotube array/polymer composites. *Composites Science and Technology*, vol. 66, pp. 387-396.

Atieh, M. A.; Girun, N. ; Mahdi, E. -S.; Tahir, H.; Guan, C. T.; Alkhatib, M. F.; Ahmadun, F. -R.; Baik, D. R. (2006): Effect of multi-wall carbon nanotubes on the mechanical properties of natural rubber. *Fullerenes, Nanotubes, and Carbon Nanostructures*, vol. 14, pp. 641-649.

Brenner, D. W.; Shederova, O. A.; Areshkin, D. A.; Schall, J. D.; Frankland, S.-J. V. (2002): Atomic modeling of carbon-based nanostructures as tool for developing new materials and technologies, *CMES: Computer Modeling in Engineering and Sciences*, vol. 3, no. 5, pp. 643-673.

Chen, W. H.; Cheng, H. C.; Hsu, Y. C. (2007): Mechanical properties of carbon nanotubes using molecular dynamics simulations with the inlayer van der waals interactions, *CMES: Computer Modeling in Engineering and Sciences*, vol. 20, no. 2, pp. 123-145.

Chen, X. L.; Liu, Y. J. (2004): Square representative volume elements for evaluating the effective material properties of carbon nanotube-based composites. *Computational Materials Science*, vol. 29, pp. 1-11.

Frankland, S. J. V.; Caglar, A.; Brenner, D. W.; Griebel, M. (2002): Molecular simulation of the influence of chemical cross-links on the shear strength of carbon

nanotube-polymer interfaces. *Journal of Physical Chemistry B*, vol. 106, pp. 3046-3048.

Franklanda, S. J. V.; Harik, V. M.; Odegard, G. M.; Brennerc, D. W.; Gatesd, T. S. (2003): The stress–strain behavior of polymer–nanotube composites from molecular dynamics simulation. *Composites Science and Technology*, vol. 63, pp. 1655–1661.

Gelin, B. R. (1994): Molecular modeling of polymer structures and properties, Hanser/Gardner Publishers.

Giannopoulos, G. I.; Kakavas P. A.; Anifantis, N. K. (2008): Evaluation of the effective mechanical properties of single walled carbon nanotubes using a spring based finite element approach. *Computational Materials Science*, vol. 41, no. 4, pp. 561-569.

Guz, A. N.; Dekret, V. A. (2009): Stability Loss in Nanotube Reinforced Composites. *Computational Materials Science*, vol. 49, no. 1, pp. 69-80.

Guz, A. N.; Rushchitsky, J. J.; Guz, I. A. (2008): Comparative Computer Modeling of Carbon-Polymer Composites with Carbon or GraphiteMicrofibers or Carbon Nanotubes. *CMES: Computer Modeling in Engineering and Sciences*, vol. 26, no. 3, pp. 139-156.

Han, Y.; Elliott, J. (2007): Molecular dynamics simulations of the elastic properties of polymer/carbon nanotube composites. *Computational Materials Science*, vol. 39, pp. 315–323.

Iijima, S. (1991): Helical microtubes of graphite carbon. *Nature*, vol. 354, pp. 56-58.

Koloczek, J.; Young-Kyun, K.; Burian, A. (2001): Characterization of spatial correlations in carbon nanotubes-modelling studies. *Journal of Alloys and Compounds*, vol. 28, pp. 222-225.

Kueseng, K.; Jacob, K. I. (2006): Natural rubber nanocomposites with SiC nanoparticles and carbon nanotubes, *European Polymer Journal*, vol. 42, pp. 220–227.

Liu, Y. J.; Chen, X. L. (2003): Continuum models of carbon nanotube-based composites using the boundary element method, *Electronic Journal of Boundary Elements*, vol. 1, pp. 316-335.

Mallick, P.K. (1988): Fiber-Reinforced Composites: Materials Manufacturing and Design, Marcel Dekker, New York, pp. 111.

Mamedv, A. A.; Kotov, N. A.; Prato, M.; Guldi, D. M.; Wicksted, J. P.; Hirsch, A. (2002): Molecular design of strong single-wall carbon nanotube/polyelectrolyte multilayer composites. *Nature Materials*, vol. 1, pp. 190-194.

Namilae, S.; Chandra, U.; Srinivasan, A.; Chandra, N. (2007): Effect of inter-

face modification on the mechanical behavior of carbon nanotube reinforced composites using parallelmolecular dynamics simulations, *CMES: Computer Modeling in Engineering and Sciences*, vol. 22, no. 3, pp. 189-202.

Odegard, G. M.; Gates, T. S.; Wise, K. E.; Park, C.; Siochi, E. (2003): Constitutive modeling of nanotube-reinforced polymer composites. *Composites Science and Technology*, vol. 63, no. 11, pp. 1671-1687.

Rappe, A. K.; Casewit, C. J.; Colwell, K. S.; Goddard W. A.; Skiff, W. M. (1992): UFF, a full periodic table force-field for molecular mechanics and molecular dynamics simulations. *Journal of American Chemical Society*, vol. 114, pp. 10024-10035.

Reich, S.; Li, L.; Robertson, J. (2005): Structure and formation energy of carbon nanotube caps. *Physical Review B*, vol. 72, pp. 165423.

Saber-Samandari, S.; Khatibi, A. A. (2006): The effect of interphase on the elastic modulus of polymer based nanocomposites. *Key Engineering Materials*, vol. 312, pp. 199-204.

Seidel, G. D.; Lagoudas, D. C. (2006): Micromechanical analysis of the effective elastic properties of carbon nanotube reinforced composites. *Mechanics of Materials*, vol. 38, pp. 884-907.

Thostenson, E. T.; Ren Z.; Chou, T. W. (2001): Advances in the science and technology of carbon nanotubes and their composites: A review. *Composites Science and Technology*, vol. 61, pp. 1899-1912.

Wang, **H. T.; Yao, Z. H.** (2009): A rigid-fiber-based boundary elementmodel for strength simulation of carbon nanotube reinforced composites. *CMES: Computer Modeling in Engineering and Sciences*, vol. 29, no. 1, pp. 1-13.

Wu, C. J.; Chou, C. Y.; Han, C. N.; Chiang, K. N. (2009): Estimation and validation of elastic modulus of carbon nanotubes using nano-scale tensile and vibrational analysis. *CMES: Computer Modeling in Engineering and Sciences*, vol. 41, no. 1, pp. 49-67.

Zou, J.; Ji, B.; Feng, X. Q.; Gao, H. (2006): Molecular-Dynamic Studies of Carbon–Water–Carbon Composite Nanotubes, *Small*, vol. 2, pp. 1348-1355.